

# Optical Properties and Structure of Indium Oxide Films Obtained Under Various Conditions of Magnetron Sputtering

© A.A. Tikhii<sup>1</sup>, Yu.M. Nikolaenko<sup>2</sup>, E.A. Sviridova<sup>2,3</sup>, I.V. Zhikharev<sup>2</sup>

<sup>1</sup> Lugansk State Pedagogical University,  
291011 Lugansk, Russia

<sup>2</sup> Galkin Donetsk Institute for Physics and Engineering,  
283048 Donetsk, Russia

<sup>3</sup> Donbass National Academy of Construction and Architecture,  
286123 Makeyevka, Russia

E-mail: ea0000ffff@mail.ru

Received July 26, 2023

Revised September 4, 2023

Accepted December 6, 2023

In this paper we summarize the studies of the structural and optical properties of  $\text{In}_2\text{O}_3$  films on  $\text{Al}_2\text{O}_3$  (012) substrates obtained by dc magnetron sputtering. According to X-ray diffraction, deposition time effects on the position and half-width of the (222) peak of cubic  $\text{In}_2\text{O}_3$ . Ellipsometric measurements and analysis of optical transmission spectra show that films obtained at temperatures of 300°C or more have uniform optical properties, except the surface layer. The refractive index of films obtained at room temperature increases along the direction from the substrate to the surface. Annealing eliminates this inhomogeneity, reduces the observed band gap due to a decrease in the concentration of lattice defects, but do not effects on the true band gap.

**Keywords:** indium oxide films, band gap, optical properties, X-ray diffraction, magnetron sputtering.

DOI: 10.61011/SC.2023.08.57619.5458

## 1. Introduction

Indium oxide films have high optical transparency and good electrical conductivity. Moreover, their electrical conductivity is sensitive to the composition of the surrounding atmosphere, and doping allows to achieve a selective response [1–4]. Thanks to this, films based on  $\text{In}_2\text{O}_3$  can be used as gas sensors. The rough surface naturally formed during the formation of these films contributes to their high sensitivity. The polycrystalline structure and mechanical stress also increase the sensitivity of such films by increasing the diffusion constants [5].

To obtain polycrystalline indium oxide films, quartz or passivated glass substrates are usually used. However, the use of sapphire substrates is justified by the better thermal and chemical stability.

Most of the works are devoted to epitaxial films on sapphire substrates [6–10], but they are rarely used to obtain polycrystalline films.

The method and modes of production have a significant influence on the surface of the film [11]. Magnetron sputtering provides higher surface roughness compared to other methods [12]. In addition, this method is scalable, provides good throughput and reproducibility, and allows the use of a wide range of substrate temperatures during the sputtering process [13,14].

Ellipsometry and optical transmittance are non-destructive optical research methods that allow non-contact investigation of the properties of nanoscale thin-film coatings. These methods complement each other, since the influence of material properties on ellipsometric measurements

decreases with distance to the surface, but for optical transmittance there is no such dependence.

In this work, we summarize the results of our previous studies of the structure and optical properties of  $\text{In}_2\text{O}_3$  films on  $\text{Al}_2\text{O}_3$  (012) substrates obtained in various modes of dc-magnetron sputtering [15–21].

## 2. Experiment

The films sputtering was carried out on an improved magnetron attachment to VUP-5M [15] at different substrate temperatures for 15–180 min. Composition of the gas environment:  $\text{O}_2$  (20%), Ar (80%). Pressure —  $10^{-2}$  Torr. Operating current — 50 mA, voltage — 300 V. The distance from the substrate to the target is — 25 mm.

The films were annealed in air for 1 hour at a temperature of 600°C.

Ellipsometric measurements were performed using a multi-angle null ellipsometer at a wavelength of  $\lambda = 632.8$  nm. Optical transmittance was measured using a Shimadzu UV-2450 spectrophotometer. X-ray diffraction measurements of targets and films were carried out on a diffractometer DRON-3.

## 3. Results and discussion

According to X-ray diffraction analysis, the films under study are polycrystalline and exhibit a peak corresponding to the (222) plane of the cubic modification  $\text{In}_2\text{O}_3$  (space group  $Ia\bar{3}$ ) [16,17].

Characteristics of In<sub>2</sub>O<sub>3</sub> films obtained at different substrate temperatures (deposition time is 1 h)

Method		Ellipsometry			Optical transmittance		
Substrate temperature, °C		20	300	600	20	300	600
Before annealing							
Parameters of the film	$n$	1.9–2	2	2.1	$0.81(n(\lambda)-1)+1-n(\lambda)$	$n(\lambda)$	$n(\lambda)$
	$k$	0	0	0	$0.81k(\lambda) - k(\lambda)$	$k(\lambda)$	$k(\lambda)$
	$d$ , nm	550	450	440	425	420	423
Parameters of the rough layer	$n$	2–1.8	2–1.53	2.1–1.6	$n(\lambda)-0.5(n(\lambda)-1)+1$	$n(\lambda)-0.1(n(\lambda)-1)+1$	$n(\lambda)-0.75(n(\lambda)-1)+1$
	$k$	0	0	0	$k(\lambda) - 0.5k(\lambda)$	$k(\lambda) - 0.1k(\lambda)$	$k(\lambda) - 0.75k(\lambda)$
	$d$ , nm	80	75	20	17	75	16
$E_g^\Gamma$ , eV					4.07	3.91	3.72
$E_g$ , eV					2.94	2.5	2.72
After annealing							
Parameters of the film	$n$	1.95	2	2.05	$n(\lambda)$	$n(\lambda)$	$n(\lambda)$
	$k$	0	0	0	$k(\lambda)$	$k(\lambda)$	$k(\lambda)$
	$d$ , nm	405	450	440	375	325	422
Parameters of the rough layer	$n$	1.87–1.67	1.8–1.5	2–1.2	$n(\lambda)-0.75(n(\lambda)-1)+1$	$n(\lambda)-0.75(n(\lambda)-1)+1$	$n(\lambda)-0.75(n(\lambda)-1)+1$
	$k$	0	0	0	$k(\lambda)-0.75k(\lambda)$	$k(\lambda)-0.75k(\lambda)$	$k(\lambda)-0.75k(\lambda)$
	$d$ , nm	21	20	30	20	20	35
$E_g^\Gamma$ , eV					3.71	3.76	3.71
$E_g$ , eV					2.69	2.43	2.67

The interpretation of the results of optical measurements of a series of films obtained at substrate temperatures of 20, 300 and 600°C was carried out taking into account the presence of surface roughness. Initially, the film material was modeled as a homogeneous isotropic layer with sharp boundaries, and the surface roughness was modeled as a layer whose optical properties vary linearly in the direction perpendicular to the sample plane. In this case, the values of the optical properties of the layer corresponding to the surface roughness are effective and depend on the fill factor. If such a model could not describe the measurement results, the change in optical properties according to a linear law was also used to describe the film material.

Ellipsometric measurements showed an increase in the thickness  $d$  and heterogeneity of the films with decreasing substrate temperature [18–20]. Thus, the refraction index  $n$  of films deposited on substrates at a temperature of 20°C increases linearly from 1.9 to 2 in the direction from the substrate to the rough layer on the surface of the film (see Table). This may be due to an increase in the surface temperature of the growing film during its deposition. An increase in the substrate temperature leads to a decrease in surface roughness, which is due to an increase in the mobility of film material particles and is consistent with

the general laws of growth of metal oxide films during magnetron sputtering [22]. The refraction index values of the rough layer at the boundaries with the film and the external environment are also given in the Table. Annealing leads to unification of the properties of the films under study and eliminates the heterogeneity of the refraction index.

Similar results were obtained based on the fringe pattern observed in the optical transmittance spectra (Figure 1). Optical transmittance spectra were calculated using the same models that were used when processing ellipsometry data. However, the spectral dependences of the refractive index  $n(\lambda)$  and the extinction coefficient  $k(\lambda)$  of the film material were taken from the work [23]. The complex refraction indices of the rough layers are calculated based on the refraction index of the film material according to the Clausius–Mossotti equation. The calculated spectra are in reasonable agreement with experimental data in the range 500–1100 nm. The discrepancy between the calculated and experimental values outside this region is associated with the onset of fundamental absorption, since the band gap of the films we studied differs slightly from the films studied by the authors of the work [23]. (This material is characterized by some scatter in the band gap values depending on the production conditions [11]).

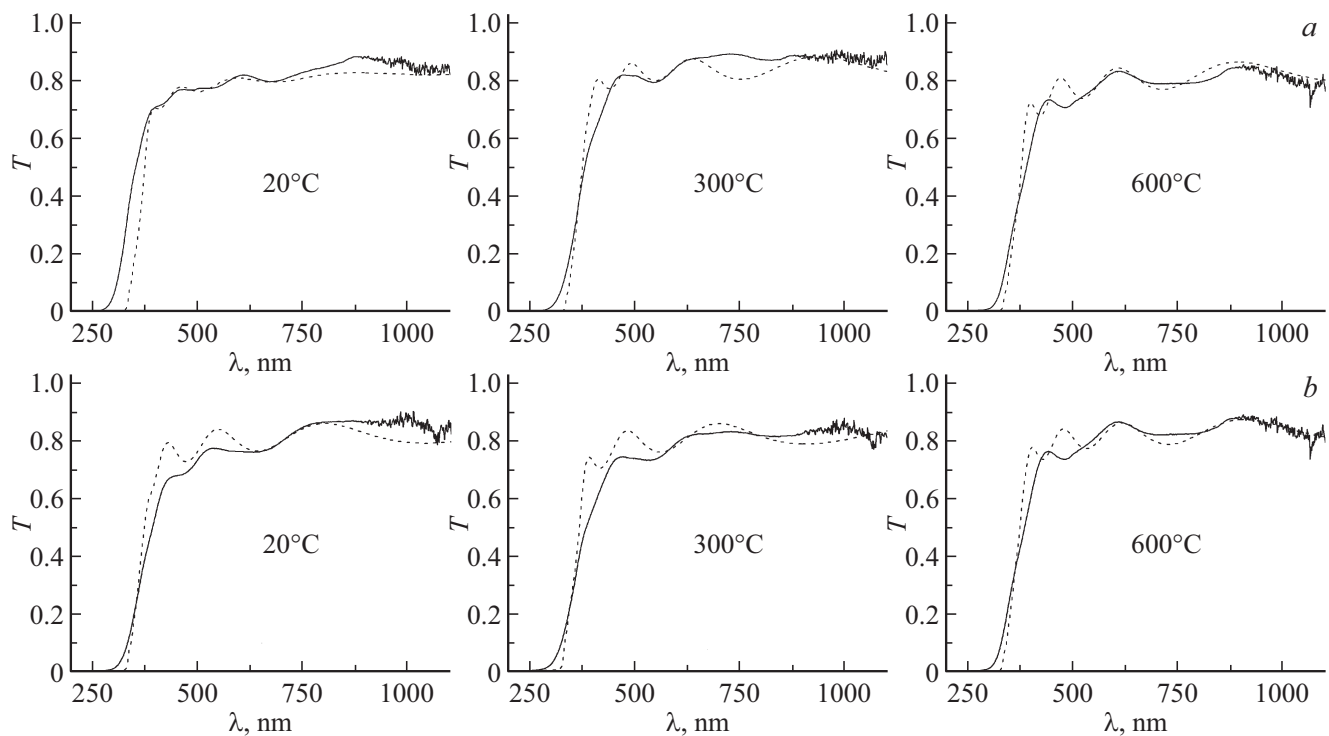


**Figure 1.** Comparison of the calculated (dashed line) and measured optical transmittance spectra (solid line) of the films under study before (a) and after annealing (b). The temperature of the substrate during the sputtering process is shown in the graphs.

The reason for the differences in layer thicknesses found from ellipsometric measurements and optical transmittance measurements may be the different nature of the sensitivity of these methods, as well as the difference in the structure of real films from the proposed model. The latter is especially likely for films obtained at room temperature. The greatest differences are in estimates of the thickness of the surface layer, since its optical properties are affected by the roughness profile, which is unknown for the samples under study.

The substrate temperature also affects the onset of fundamental absorption [18–20]. The observed band gap  $E_g^\Gamma$  decreases with increasing temperature.  $E_g^\Gamma$  also decreases as a result of annealing. This is well explained by the model of the band structure  $\text{In}_2\text{O}_3$  presented in the work [24]. According to this model, the observed direct band gap differs significantly from the real one due to lattice symmetry and the Burstein–Moss shift. The latter significantly depends on the defectiveness of the crystal structure. The number of defects is lower in films deposited on substrates at higher temperatures. Annealing in air eliminates oxygen vacancies. In turn, this reduces the concentration of charge carriers and the value of  $E_g^\Gamma$  [25,26]. The band gap for symmetry-forbidden transitions  $E_g$  changes less due to electron-phonon interactions.

The structure of some studied films obtained at the substrate temperature  $600^\circ\text{C}$  depends on the sputtering time [21]. Thus, according to X-ray diffraction data, the reflection corresponding to the (222) plane  $\text{In}_2\text{O}_3$

shifts from  $30.3$  to  $30.6^\circ$  with decreasing sputtering time. Meanwhile, its half-width decreases.

The optical transmittance of such films decreases anomalously with decreasing wavelength. To describe their optical properties, we used a three-layer model (Figure 2). The first layer of this model describes the rough surface of the film as a homogeneous layer with optical properties calculated on the basis of the dielectric constant of the cubic modification  $\text{In}_2\text{O}_3$  and a fill coefficient of 0.5, in accordance with the Clausius–Mossotti equation. The optical properties of the second layer correspond to the cubic modification of  $\text{In}_2\text{O}_3$  according to [23]. The third layer is characterized by a high extinction coefficient and is located between the film and the substrate. The spectrum of the extinction coefficient of this layer is described by the law of intrinsic absorption of the semiconductor with  $E_g^\Gamma = 1.39$  eV. According to ellipsometric measurements, its refractive index is close to 3. This is consistent with the calculated refractive index of a semiconductor with a band gap of 1.39 eV, according to [27].

Figure 3 shows that the thickness of the surface layer decreases, and the thickness of the middle layer increases with increasing sputtering time up to 60 min, while the total thickness of the film remains almost unchanged. This indicates that films with longer sputtering times contain, on average, smaller crystallites. Thus, it can be assumed that large particles of material are formed on the surface of the substrate at the beginning of sputtering, and then during the sputtering process the size of the resulting crystallites decreases and they fill the gaps between larger particles.

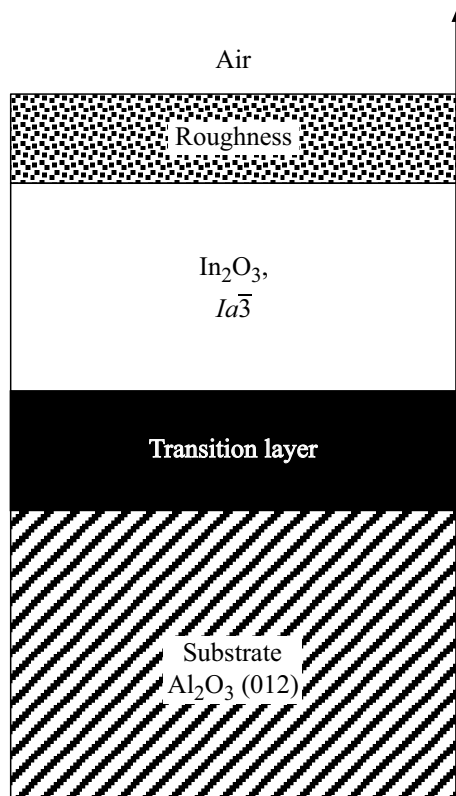


Figure 2. Three-layer model of the films under study.

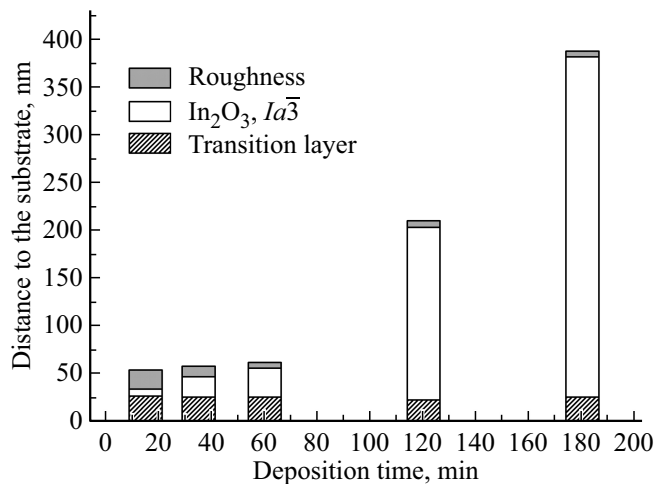


Figure 3. Structures of films in a series with different deposition times.

Subsequently (60–180 min), the thickness of the surface layer is maintained with an increase in the total thickness of the film — the process of film formation reaches a steady state mode.

The transition layer at the interface with the substrate is probably formed as a result of the presence of impurity levels inside the band gap and its blurring due to a large number of defects in the crystal structure. Since its thickness is practically independent of the sputtering time,

the appearance of this layer is entirely due to the influence of the substrate surface.

## 4. Conclusion

The observed band gap of the studied films decreases with increasing substrate temperature during sputtering. Annealing also reduces the observed band gap. This, as well as the differences in refraction indices, thicknesses and roughness of the films, is explained by the elimination of defects in the crystal structure under the influence of high temperatures in the presence of oxygen. The obtained band gap values are consistent with the results obtained by other authors [11,22–25].

The optical properties of some In<sub>2</sub>O<sub>3</sub> films indicate the presence of an additional layer with a band gap of 1.39 eV and a refraction index of 3 at the interface with the substrate. Also, as such films grow, the size of the crystallites changes — first, large particles of material are formed on the surface of the substrate, then the spaces between them are filled with smaller crystallites, and the process reaches a steady state mode.

## Conflict of interest

The authors declare that they have no conflict of interest.

## References

- [1] A.A. Yousif, M.H. Hasan, J. Biosens. Bioelectron, **6**, 1000192 (2015).
- [2] J. Liu, W. Guo, F. Qu, C. Feng, C. Li, L. Zhu, J. Zhou, S. Ruan, W. Chen. Ceramics International, **40**, 6685 (2014).
- [3] A.A. Khalefa, J.M. Marei, H.A. Radwan, J.M. Rzaizj. Digest J. Nanomater. Biostructures, **16**, 197 (2021).
- [4] D. Manno, M.D. Giulio, T. Siciliano, E. Filippo, A. Serra. J. Phys. D: Appl. Phys., **34**, 2097 (2001).
- [5] Yu.M. Nikolaenko, A.N. Artemov, Yu.B. Medvedev, N.B. Efros, I.V. Zhikharev, I.Yu. Reshidova, A.A. Tikhii, S.V. Kara-Murza. J. Phys. D: Appl. Phys., **49**, 375302 (2016).
- [6] S. Kaneko, H. Torii, M. Soga, K. Akiyama, M. Iwaya, M. Yoshimoto, T. Amazawa. Jpn. J. Appl. Phys., **51**, 01AC02 (2012).
- [7] S.K. Yadav, S. Das, N. Prasad, B.K. Barick, S. Arora, D.S. Sutar, S. Dhar. J. Vacuum Sci. Technol. A, **38**, 033414 (2020).
- [8] X. Du, J. Yu, X. Xiu, Q. Sun, W. Tang, B. Man. Vacuum, **167**, 1 (2019).
- [9] M. Nistor, W. Seiler, C. Hebert, E. Matei, J. Perrière. Appl. Surf. Sci., **307**, 455 (2014).
- [10] W. Seiler, M. Nistor, C. Hebert, J. Perrière. Solar Energy Mater. Solar Cells, **116**, 34 (2013).
- [11] M.Z. Jarzebski. Phys. Status Solidi A, **71**, 13 (1982).
- [12] H. Kim, C.M. Gilmore, A. Pique, J.S. Horwitz, H. Mattoussi, H. Murata, Z.H. Kafafi, D.B. Chrisey. J. Appl. Phys., **86**, 6451 (1999).
- [13] M. Higuchi, S. Uekusa, R. Nakano, K. Yokogawa. J. Appl. Phys., **74**, 6710 (1993).

- [14] Y. Shigesato, S. Takaki, T. Haranoh. *J. Appl. Phys.*, **71**, 3356 (1992).
- [15] Yu.M. Nikolaenko, A.B. Mukhin, V.A. Chaika, V.V. Burkhovetskii. *Techn. Phys.*, **55** (8), 1189 (2010).
- [16] A.A. Tikhii, Yu.M. Nikolaenko, Yu.I. Zhikhareva, I.V. Zhikharev. In: *7th Int. Congress on Energy Fluxes and Radiation Effects* (EFRE-2020 online): Abstracts (Tomsk, Publishing House of IAO SB RAS, 2020) p. 601.
- [17] A.A. Tikhii, Yu.M. Nikolaenko, Yu.I. Zhikhareva, I.V. Zhikharev. *Opt. Spectrosc.*, **128** (10), 1667 (2020).
- [18] A.A. Tikhii, Yu.M. Nikolaenko, Yu.I. Zhikhareva, A.S. Kornievets, I.V. Zhikharev. *Semiconductors*, **52**, 320 (2018).
- [19] V.A. Gritskikh, I.V. Zhikharev, S.V. Kara-Murza, N.V. Korchikova, T.V. Krasnyakova, Y.M. Nikolaenko, A.A. Tikhii, A.V. Pavlenko, Y.I. Yurasov. In: *Advanced Materials Techniques, Physics, Mechanics and Applications* [(Eds I.A. Parinov, S.-H. Chang, M.A. Jani), Springer Proceedings in Physics. V. 193 (Springer International Publishing AG., 2017) p. 55].
- [20] A.A. Tikhii, V.A. Gritskikh, S.V. Kara-Murza, N.V. Korchikova, Yu.M. Nikolaenko, Yu.I. Zhikhareva, I.V. Zhikharev. In: *European Materials Research Society Spring Meeting 2016* (E-MRS 2016) (Lille, France, 2016) L.P. 32. <https://www.european-mrs.com/2016-spring-symposium-l-european-materials-research-society>, date of access: July, 2023
- [21] A.A. Tikhii, K.A. Svyrydova, Yu.I. Zhikhareva, I.V. Zhikharev. *J. Appl. Spectrosc.*, **88** (5), 975 (2021).
- [22] E. Kusano. *Appl. Sci. Converg. Technol.*, **28** (6), 179 (2019).
- [23] A. Schleife, M.D. Neumann, N. Esser, Z. Galazka, A. Gottwald, J. Nixdorf, R. Goldhahn, M. Feneberg. *New J. Phys.*, **20**, 053016 (2018).
- [24] A. Walsh, J.L.F. Da Silva, S.-H. Wei, C. Korber, A. Klein, L.F.J. Piper, A. De Masi, K.E. Smith, G. Panaccione, P. Torelli, D.J. Payne, A. Bourlange, R.G. Egdell. *Phys. Rev. Lett.*, **100**, 167402 (2008).
- [25] Y. Furubayashi, M. Maehara, T. Yamamoto. *ACS Appl. Electron. Mater.*, **1**, 1545 (2019).
- [26] L. Gupta, A. Mansingh, P.K. Srivastava. *Thin Sol. Films*, **176**, 33 (1989).
- [27] N.M. Ravindra, P. Ganapathy, J. Choi. *Infr. Phys. Technol.*, **50**, 21 (2007).

*Translated by Ego Translating*